A Review of Point Target Spectra for Bistatic SAR Processing.

Yewlam Neo
DSO National Labs. at Singapore, Singapore

Frank Wong
MacDonald Dettwiler and Associates at Richmond, British Columbia, Canada

Ian Cumming
The University of British Columbia at Vancouver, British Columbia, Canada

Abstract

Bistatic SAR data are more complicated to process than monostatic data because of the versatile sensor geometry and the non-stationary properties of the received data. Recent approaches to the processing of bistatic SAR data have revolved around finding an accurate representation of the two-dimensional spectrum for a point target.
In this paper, we review past methods of obtaining the spectrum, then present a new method based on a power series. We then establish the relationship between three independently-derived bistatic point target spectra. The first spectrum is Loffeld's Bistatic Formula (LBF), which consists of a quasi-monostatic phase term and a bistatic phase term. The second spectrum makes use of Rocca's smile operator, which transforms bistatic data in a defined configuration to a monostatic equivalent. The third spectrum is derived using the method of series reversion (MSR). Simulations are performed to illustrate the focusing accuracies of each form of the spectrum.

1 Introduction

The formulation of a point target spectrum is a key step in deriving SAR focusing algorithms that exploits the processing efficiency of the frequency domain [1]. The general bistatic SAR range equation has a Double Square Root (DSR) term. This term makes it difficult to apply the method of stationary phase [2] directly in order to obtain an analytical solution for the two-dimensional spectrum. A survey of the literature shows that there are three generic approaches to dealing with this inversion problem.

The first method is to solve the problem numerically [3, 4]. These algorithms are similar to the monostatic $\omega - k$ algorithm [5] except that they make use of numerical methods when calculating the DSR phase term. Bamler et al. [6] proposed a focusing algorithm that replaces the analytical SAR transfer functions with numerical equivalents. The second approach is to transform the bistatic data to a monostatic equivalent. In [7], a convolution phase term called the Rocca's smile operator was used to perform this step. This method is limited to processing the stationary bistatic case[1] where the receiver and transmitter have identical velocities and flight paths (tandem case). A method is suggested for the azimuth-variant case in [8].

The third method is to solve for the two-dimensional spectrum directly using the method of stationary phase. An approximate analytical solution for the general bistatic two-dimensional frequency spectrum has been proposed in [9]. Recently, a power series method for the general bistatic case has been formulated. The spectrum of a single point target is derived based on the method of series reversion [10]. This method gives an accurate formulation of the stationary point in the form of a power series.

This paper shows the relationships between three methods used to derive the two-dimensional bistatic spectrum, the LBF method, Rocca's smile operator and the MSR. Simulation results are used to illustrate the accuracy of the algorithms, when the transmitting and receiving aircrafts have non-equal velocities, and non-parallel flight paths. In particular, the simulation for the non-parallel flight path is based on the geometry used in the bistatic exploration project involving the TerraSAR-X satellite with airborne SAR sensor PAMIR.

2 Point Target Spectra

The point target spectrum used in this paper is based on a 2-D spectrum of the reference point target derived in [10] and repeated here for convenience:

$$S(f_\tau, f_\eta) \approx W_{\mathrm{r}}(f_\tau)\ W_{\mathrm{az}}\left(f_\eta + (f_{\mathrm{o}} + f_\tau)\frac{k_1}{c}\right) \exp\left\{-j\left[\phi_{\mathrm{T}}\big(\eta(f_\eta)\big) + \phi_{\mathrm{R}}\big(\eta(f_\eta)\big)\right]\right\} \quad (1)$$

[1] In this context, the term "stationary" refers the the bistatic geometry being constant with azimuth time.

where $W_{\rm r}$ represents the spectral shape of the transmitted pulse and $W_{\rm az}$ represents the shape of the received Doppler spectrum. The parameter, k_1, is the first derivative of the expanded range equation in azimuth time η, given in [10]. The variable, f_η, is the azimuth frequency, f_τ is the range frequency, $f_{\rm o}$ is the carrier frequency and c is the speed of light. The variable, $\eta(f_\eta)$, contains the relationship between azimuth frequency, f_η, and azimuth time, η, found by solving for the stationary phase point.
The variable, ϕ_T, is the transmitter-based phase term and ϕ_R the receiver-based phase term in the spectrum (1), given by

$$\phi_{\rm T}(\eta) \;=\; 2\pi\,\frac{(f_{\rm o}+f_\tau)}{c}\,R_{\rm T}(\eta) \;+\; \pi f_\eta\,\eta \qquad (2)$$

$$\phi_{\rm R}(\eta) \;=\; 2\pi\,\frac{(f_{\rm o}+f_\tau)}{c}\,R_{\rm R}(\eta) \;+\; \pi f_\eta\,\eta \qquad (3)$$

where R is the instantaneous range to the point target, and the subscripts, T and R, refer to the transmitter and receiver, respectively. The two range functions, $R_{\rm T}$ and $R_{\rm R}$, have a hyperbolic form and the sum of the two functions gives rise to the DSR form of the bistatic range function, R. For simplicity, we have dropped the f_η dependence of η in these and subsequent equations.
While an approximate analytical solution exists for $\eta(f_\eta)$ in the monostatic case, no simple analytical solution is available for this time-frequency relationship in the bistatic case. The problem lies in the inversion of the DSR. In the following subsections, we examine briefly how two bistatic spectra [9, 10] handle the inversion problem.

2.1 Method of Series Reversion (MSR)

The MSR method expands the phase history around the beam center at zero azimuth time, the time that the composite beam center crosses the target. The MSR first expands the instantaneous bistatic range, $\mathrm{R}(\eta)$, in azimuth time as a Taylor series around $\eta = 0$. Solving for the bistatic stationary phase point by using the series reversion formula, we obtain a power series representation of $\eta(f_\eta)$ which we denote by $\widetilde{\eta}_{\rm b}$

$$\widetilde{\eta}_{\rm b} \;=\; A_1\left(-\frac{c\,f_\eta}{f_{\rm o}\,+\,f_\tau}\,-\,k_1\right)\;+\;A_2\left(-\frac{cf_\eta}{f_{\rm o}\,+\,f_\tau}\,-\,k_1\right)^2\;+\;\ldots \qquad (4)$$

The accuracy of this spectrum is affected by the number of terms used in the expansion of (4). This is a key feature of the MSR formulation. For a higher resolution, a wider aperture or a larger bistatic angle, more phase terms need to be retained to achieve a specified level of accuracy in the spectrum, as illustrated by an example in [10].

2.2 Loffeld's Bistatic Formulation (LBF)

Loffeld et al. derived an approximate analytical solution for the point target response in the two-dimensional frequency domain by applying a Taylor series expansion to the one-way phase terms, $\phi_{\rm T}(\eta)$ and $\phi_{\rm R}(\eta)$, in (2) and (3) [9]. The monostatic phase functions are expanded about their individual monostatic stationary phase points up to the second order phase term,
Applying the method of stationary phase, the approximate stationary phase point is given by $\widehat{\eta}_{\rm b}$

$$\widehat{\eta}_{\rm b} \;=\; \frac{\ddot{\phi}_{\rm T}(\widetilde{\eta}_{\rm T})\,\widetilde{\eta}_{\rm T}\;+\;\ddot{\phi}_{\rm R}(\widetilde{\eta}_{\rm R})\,\widetilde{\eta}_{\rm R}}{\ddot{\phi}_{\rm T}(\widetilde{\eta}_{\rm T})\;+\;\ddot{\phi}_{\rm R}(\widetilde{\eta}_{\rm R})} \qquad (5)$$

and the spectrum is given by

$$S_2(f_\tau,f_\eta) \;\approx\; W_{\rm r}(f_\tau)\;W_{\rm az}\!\left(f_\eta+(f_{\rm o}+f_\tau)\frac{k_1}{c}\right)\exp\{-j\Psi_1(f_\tau,f_\eta)\}\;\exp\left\{-\frac{j}{2}\Psi_2(f_\tau,f_\eta)\right\} \qquad (6)$$

The first exponential term, Ψ_1, is known as the quasi-monostatic term while the second exponential term, Ψ_2, is known as the bistatic deformation term. Unlike the MSR formulation of Section 2.1, the accuracy of this spectrum is restricted by the limiting the number of phase terms up to the second order.
MSR can also be expanded about the two monostatic stationary point to give the Two-Stationary Phase Points (TSPP) method [11]. The quasi-monostatic term of the TSPP and LBF are identical. The bistatic deformation component for the LBF is an analytical term. In contrast, the bistatic deformation term for the TSPP is given by a power series.

3 Simulation 1

In this section, we simulate three equal-velocity, parallel-track, stationary cases with both platforms operating in stripmap mode, to compare and verify the accuracy of the point target spectra between the LBF, TSPP and the MSR methods.
For the first case, the platform velocity are both 98 m/sec with a center frequency of 10.17 GHz. Range bandwidth of 50 MHz and Doppler bandwidth of 660 Hz. The geometry of the flight path is altitude 1000 m, baseline 2000 m with Range to point target of 3794 and 1999 m and squint angles of 10° and 19.25° for the transmitter and receiver respectively.

3.1 Simulation 1 Results

The azimuth impulse responses are shown in Figure 1. The point target focused using the LBF in Figure 1(a) is not well focused. Figure 1(b) shows the same point target focused using the TSPP spectrum, expanded up to the quadratic term. While there is less degradation in Figure 1(b) compared with Figure 1(a), an improved result

can be obtained by including the cubic phase term in the expansion — as shown in Figure 1(c).

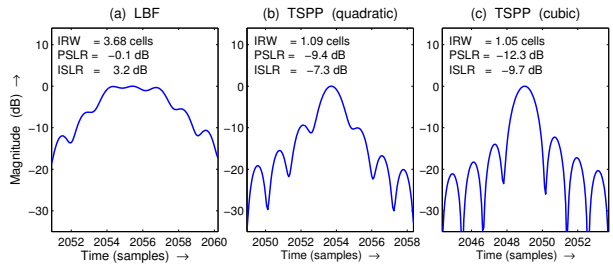

Figure 1: Azimuth impulse responses: (a) using the LBF, (b) using the TSPP, up to the quadratic term, (c) using the TSPP, up to the cubic term.

4 LBF and DMO

The existence of the quasi-monostatic and bistatic phase terms suggests a two-step focusing approach: the removal of the bistatic deformation followed by the application of a quasi-monostatic focusing step [9]. Such a method is similar to the Dip Move Out (DMO) algorithm put forward by D'Aria et al. that uses Rocca's smile operator [7]. In this section, a geometrical proof is given to show how the LBF bistatic deformation term is linked to the Rocca's smile operator for the tandem configuration.

4.1 The Link Between LBF and Rocca's Smile Operator

A geometrical method borrowed from seismic reflection surveying [7], is used to transform a bistatic configuration to a monostatic one. The bistatic platforms are restricted to travelling on the same path with constant and equal velocities, as illustrated in Figure 2. This stationary bistatic case is known as the tandem configuration.

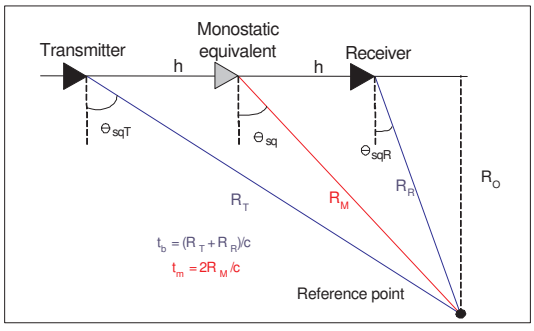

Figure 2: Geometry of the bistatic tandem configuration.

For this tandem case, Rocca's smile operator transforms the bistatic data to a monostatic equivalent, which corresponds to a single platform located at the mid-point of the two bistatic platforms. To do this transformation, a range shift and phase compensation are required — the shift corresponds to the time difference between the two geometries. The time difference is denoted by t_{DMO}, given by

$$t_{\mathrm{DMO}}(\theta_{\mathrm{sq}}) \;=\; t_{\mathrm{b}}(\theta_{\mathrm{sq}}) \;-\; t_{\mathrm{m}}(\theta_{\mathrm{sq}}) \qquad (7)$$

where t_{b} is the bistatic round-trip travel time from the transmitter to the point target back to the receiver and t_{m} is the round-trip travel time between the equivalent monostatic antenna and the point target.

It can be shown that the travel times are related by

$$t_{\mathrm{b}}^2(\theta_{\mathrm{sq}}) \;\approx\; t_{\mathrm{m}}^2(\theta_{\mathrm{sq}}) \;+\; \frac{4h^2}{c^2}\cos^2\theta_{\mathrm{sq}} \qquad (8)$$

$$t_{\mathrm{DMO}}(\theta_{\mathrm{sq}}) \;\approx\; \frac{2h^2\cos^2\theta_{\mathrm{sq}}}{c^2\, t_{\mathrm{b}}} \qquad (9)$$

The bistatic platforms are at a constant offset of $2h$ from each other and θ_{sq} is the squint angle of the equivalent monostatic configuration.
From the derivations given in [7], we have the following observations. The bistatic configuration can be transformed to the monostatic configuration by applying small negative delays t_{DMO} as a function of monostatic squint, θ_{sq}. Applying these negative delays is akin to convolving the bistatic data with the smile operator (the "negative delays" *decrease* t_{b} to t_{m}). It was shown that the **smile operator** in the two-dimensional frequency domain for the constant offset case is [7]

$$H(f_\tau, f_\eta) \;\approx\; \exp\left\{ j2\pi(f_{\mathrm{o}} + f_\tau)\, t_{\mathrm{DMO}}(\theta_{\mathrm{sq}}) \right\} \qquad (10)$$

5 Simulation 2

In this section, we simulate three equal-velocity, parallel-track, stationary cases with both platforms operating in stripmap mode, to compare and verify the accuracy of the point target spectra between the LBF, TSPP and the MSR methods.
For this simulation, the platform velocity are both 100 m/sec with a center frequency of 10.17 GHz. Range bandwidth of 50 MHz and Doppler bandwidth of 232 Hz. The geometry of the flight path - tandem flight configuration with altitude 1000 m, baseline 3000 m with Range to point target of 4026 m and 4026 m and squint angles of $-21.8°$ and $21.8°$ for the transmitter and receiver respectively.

5.1 Simulation 2 Results

Figure 4(a) shows that Rocca's smile method is not able to focus the point target with this large baseline. Also, Figure 4(b) shows that the focusing limits of the LBF are also reached at this baseline. Figure 4(c) shows that the MSR

is still able to focus this symmetrical, large baseline data correctly, by expanding the spectrum up to the fourth order azimuth frequency term.

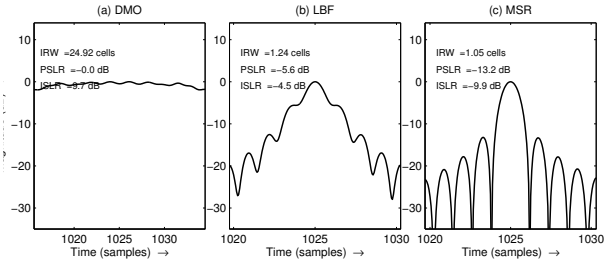

Figure 4: Azimuth impulse responses: (a) using the DMO, (b) using the LBF, (c) using the MSR.

6 Simulation 3

In this section, we simulate the satellite-airborne configuration similar to [12] to compare the accuracy of the point target spectra between the LBF and the MSR methods.
For this simulation, the center frequency is 9.65 GHz, range bandwidth is 300 MHz and Doppler bandwidth is 1230 Hz. the TerraSAR satellite has an altitude of 515 km and a velocity of 7600 m/sec while PAMIR has a velocity of 100 m/sec and an altitude of 3km. The point target is at the scene center with a bistatic angle of 30°.

6.1 Simulation 3 Results

Figure 5(a) shows that LBF is not able to focus the point target. Figure 5(b) shows that the focusing shows that the MSR is still able to focus this configuration by expanding the phase term up to the fourth order azimuth frequency term.

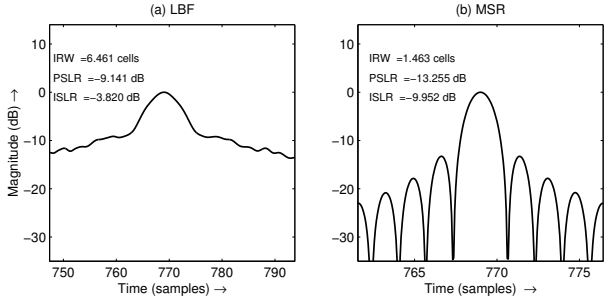

Figure 5: Azimuth impulse responses: (a) using the LBF, (b) using the MSR

References

[1] I. G. Cumming and F. H. Wong. *Digital Processing of Synthetic Aperture Radar Data: Algorithms And Implementation*. Artech House, Norwood, MA, 2005.

[2] A. Papoulis. *Signal Analysis*. McGraw-Hill, New York, 1977.

[3] I. Walterscheid, J. H. G. Ender, A. R. Brenner, and O. Loffeld. Bistatic SAR Processing and Experiments. *IEEE Trans. Geoscience and Remote Sensing*, Vol. 44(10): pp. 2710–2717, October 2006.

[4] V. Giroux, H. Cantalloube, and F. Daout. An Omega-K algorithm for SAR bistatic systems. In *Proc. Int. Geoscience and Remote Sensing Symp., IGARSS'05*, Seoul, Korea, August 2005.

[5] C. Cafforio, C. Prati, and F. Rocca. Full Resolution Focusing of SEASAT SAR Images in the Frequency-Wave Number Domain. In *Proc. 8th EARSel Workshop*, pages 336–355, Capri, Italy, May 17–20, 1988.

[6] R. Bamler, F. Meyer, and W. Liebhart. Processing of Bistatic SAR Data From Quasi-Stationary Configurations. *IEEE Trans. Geoscience and Remote Sensing*, 45: pp. 3350–3358, November 2007.

[7] D. D'Aria, A. M. Guarnieri, and F. Rocca. Focusing Bistatic Synthetic Aperture Radar using Dip Move Out. *IEEE Trans. on Geoscience and Remote Sensing*, 42(7): pp. 1362–1376, 2004.

[8] A. Monti Guarnieri and F. Rocca. Reduction to monostatic focusing of bistatic or motion uncompensated SAR surveys. *IEE Proc. Radar, Sonar and Navigation*, Vol. 153(3):254–261, June 2006.

[9] O. Loffeld, H. Nies, V. Peters, and S. Knedlik. Models and Useful Relations for Bistatic SAR Processing. *IEEE Trans. on Geoscience and Remote Sensing*, 42(10): pp. 2031–2038, October 2004.

[10] Y. Neo, F. H. Wong, and I. G. Cumming. A two-dimensional spectrum for bistatic SAR processing using series reversion. *IEEE Geoscience and Remote Sensing Letters*, 4(1): pp. 93 – 96, January 2007.

[11] Y. Neo, F. H. Wong, and I. G. Cumming. A Comparison of Point Target Spectra Derived for Bistatic SAR Processing. Accepted by *IEEE Trans. on Geoscience and Remote Sensing*.

[12] I. Walterscheid,T. Especter and J. H. G. Ender Performance Analysis of a Hybrid Bistatic SAR System Operating in the Double Sliding Spotlight-Mode In *Proc. Int. Geoscience and Remote Sensing Symp., IGARSS'07*, Barcelona, Spain, July 2006. [CD-ROM]